Spatiotemporal model for the progression of sand blowouts

H. Yizhaq

Department of solar Energy and Environmental Physics, BIDR, Ben-Gurion University, Midreshet Ben-Gurion, Israel

Y. Ashkenazy

Department of solar Energy and Environmental Physics, BIDR, Ben-Gurion University, Midreshet Ben-Gurion, Israel

H. Tsoar

Department of Geography and Environmental Development, Ben-Gurion University, Beer Sheva, Israel

N. Levin

Department of Geography, The Hebrew University, Jerusalem, Israel

H. Yizhaq, Solar Energy and Environmental Physics, BIDR, Ben-Gurion University, Midreshet Ben-Gurion 84990, Israel. (yiyeh@bgu.ac.il)

Abstract. Sand blowouts (surrounded by vegetation) exist in many coasts. In some regions, small blowouts shrink while large ones grow, although both experience the same climatic conditions. We propose a mathematical model for the spatiotemporal dynamics of vegetation cover on sand dunes and focus on the dynamics of sand blowouts (and transgressive dunefields). Among other possibilities, the model predicts blowout growth parallel to the wind with shrinkage perpendicular to the wind, where, depending on geometry and size, a blowout can initially grow although eventually shrink. The model's predictions are supported by field observations from Fraser Island in Australia.

1. Introduction

Sand dunes cover a vast area of Earth land surface. Their formation and dynamics were challenged by researchers, as their complex nature may be formulated mathematically based on physical principles. While several mechanisms/models for the development of dunes have been proposed [*Bagnold*, 1941; *Andreotti et al.*, 2002; *Durán and Herrmann*, 2006; *Luna et al.*, 2009; *Reitz et al.*, 2010], the dynamics of blowouts and transgressive dunefields received lesser attention, in spite of its ecological, climatological, and anthropogenic importance. For example, field observations indicate [*Pye*, 1982] that, in spite the same climatic conditions, large blowouts grow while small ones shrink and some show sign of narrowing after an initial phase of widening phase.

Below we present a spatiotemporal model for large scale sand dune dynamics, where the dependant variable is the vegetation cover. This variable is associated with the stability of dune—active/fixed dunes have small/large vegetation cover. We use this model to study the dynamics of blowouts and of transgressive dunes.

Transgressive dunes are relatively large sand bodies, which can migrate perpendicular to shore, obliquely landwards or alongshore [*Martinho et al.*, 2010]. The dunefield margins are often formed by ridges of sand "precipitation" into vegetation [*Hesp and Martínez*, 2007]. Basically, sand "rains" down onto the adjacent vegetation by grain-fall, avalanche, and saltation, forming a steep slope, often lying at the angle of repose ($\sim 33^\circ$). Blowouts are trough-shaped depressions formed by wind erosion of a sandy substrate [*Hesp and Martínez*, 2007]. Blowouts can be formed after plant destruction by, e.g., fire or human activity; as a result, bare sand is exposed to wind erosion. Typical blowout area is 100–10^5

m^2. Blowouts usually propagate downwind and the vegetation at the downwind side is inundated with sand and often completely smothered and killed.

One of the complex behaviors associated with dune dynamics is dune bistability; i.e., under similar climatic conditions it is possible to find both active and fixed dunes [*Yizhaq et al.*, 2007, 2009]. The propagation of the border (front) between active and fixed dune areas depends mainly on rainfall wind power and wind direction. Blowout dynamics may be determined by the dynamics of the fronts separating it from the vegetated background (see, e.g., Fig. 1a). These fronts are the transitions zones that separate in space alternative stable uniform states. The dynamics of the whole pattern depend on the dynamics of individual fronts and on the interactions between adjacent fronts. Along the wind direction two fronts may be identified: (i) the fixed-active (FA) front which connects the upwind fixed (vegetated) area with the downwind active (bare) area and the (ii) active-fixed (AF) front which connects the active upwind area with the downwind fixed area. The cross wind fronts separate the active dunes from the vegetated dunes perpendicular to the wind direction. In the following discussion we refer to blowouts that are not connected to the beach which can only grow downwind. There are four possibilities of blowout dynamics, depending on the fronts propagation velocities: (i) An initial blowout grows both along and perpendicular to the wind direction, (ii) an initial blowout grows along the wind but shrinks perpendicular to the wind, (iii) an initial blowout grows perpendicular to the wind but shrinks along the wind, and (iv) an initial blowout shrinks in both directions.

Such dynamics of blowouts has been observed in Fraser Island [*Levin*, 2011]. While most of Fraser Island's (Australia) dunes are fixed and covered by forests, there are dozens of active blowouts [*Levin*, 2011]. Using aerial photos and satellite images, changes (since

1940) in the area of 70 blowouts were measured by Levin [*Levin*, 2011]. The overall trend (Fig. 2) is of dune stabilization, i.e., reduction in blowouts area, being more pronounced in the smaller blowouts and in blowouts which were detached from the beach and had no fresh supplies of sand. Although the overall sand drift potential (DP, defined below) by the wind in this area is high (DP$\sim$490 for 1997-2006, based on NCDC hourly database (www.ncdc.noaa.gov) and NCEP/NCAR [*Kalnay et al.*, 1996] and ECMWF [*Uppala et al.*, 2005] reanalysis), the dunes are stabilizing. This stabilization was attributed to reduction in wind power and tropical cyclone activity [*Levin*, 2011].

The goal of this paper is to explain part of the dynamics of transgressive dune field and blowouts, including the observation of faster stabilization of smaller blowouts as shown in Fig. 2. To this end we develop a physically motivated spatiotemporal model for dune field dynamics. The proposed model predicts parameter values that allow both growth and shrink of blowouts, depending on the blowout initial area and geometry.

2. Model

Empirical studies have shown that dune activity can be modeled successfully using wind power and vegetation cover [*Hugenholtz and Wolfe*, 2005], as wind power may be associated with sand transport, while vegetation cover may be linked to the amount of the sand available for transport. Recently, we developed a simple model for the development of vegetation cover on dunes as a function of wind power and rainfall [*Yizhaq et al.*, 2007, 2009]. That model has only temporal dynamics and exhibits bistability and hysteresis mainly with respect to wind power and precipitation. The model proposed here has both spatial and temporal dynamics, including wind directionality. The wind magnitude

and direction play an important role in the development of the model's variable, as is the case for dune formation [*Fryberger*, 1979].

Following [*Yizhaq et al.*, 2007, 2009], we propose a model with a single variable, the vegetation dune cover density v:

$$\begin{aligned}\frac{\partial v}{\partial t} &= \alpha(p)(v+\eta)\left(1-\frac{v}{v_{\max}}\right)-\varepsilon \mathrm{DP} g(v_c,v)v \\ &-\gamma \mathrm{DP}^{2/3}v-\mu v+\beta \mathrm{DP}\frac{\partial g(v_c,v)}{\partial v}\left|\nabla v\cdot\vec{k}\right|v \\ &-\kappa \mathrm{DP}^{2/3}(\nabla v\cdot\vec{k})v+\delta\nabla^2 v\,. \end{aligned} \quad (1)$$

The vegetation cover $v(x,y,t)$ depends on time t, and space, x and y, and is bounded between 0 (bare dune) and $v_{\max} \leq 1$. The first term on the RHS represents vegetation logistic growth. This term includes a spontaneous growth rate η that represents spontaneous growth even for bare dunes due to soil seed banks, underground roots, seeds carried by wind, animals, etc. The growth rate constant, α, depends on precipitation

$$\alpha(p)=\begin{cases}\alpha_{\max}(1-\exp(-(p-p_{\min})/c)) & p\geq p_{\min}\\ 0 & p<p_{\min}\end{cases}, \quad (2)$$

where $p_{\min}$ is ∼50 mm/yr [*Tsoar*, 2005]. For high precipitation rate the growth rate converges to a maximal value α_{max} in accordance with observations [*Shmida et al.*, 1986].

The next term in Eq. (1), $-\varepsilon \mathrm{DP} g(v_c,v)v$, represents the destructive effect of sand transport on vegetation, mainly due to root exposure and plant burial. Because saltating particles carry most of the mass and momentum, it can have considerable physical effects on existing vegetation, exposure of below ground plant tissue (pedastaling), abrasion of plant tissue, and leaf stripping. This effect has been shown to indirectly leading to reduced plant growth and mortality [*Field et al.*, 2010]. v_c is the critical vegetation cover

above which the sand is protected from the wind [*Wolfe and Nickling*, 1993, 1996] (v_c is associated with a skimming flow pattern) and it varies, typically from 0.14 to 0.35, for different geographical locations and for different vegetation types as plants are porous objects [*Okin*, 2008] and each plant has a different porosity to wind flow. The drift potential, DP, is DP $=\langle U^2(U-U_t)\rangle$, where U is the wind speed (in knots: 1 knot = 0.514 m/s) at 10 m height and U_t is a minimal threshold velocity (= 12 knots) necessary for sand transport [*Fryberger*, 1979]. There are both theoretical and empirical linear relations between DP and the rate of sand transport [*Bullard*, 1997]. We use a (step-like) hyperbolic function for $g(v_c, v)$ in Eq. (1)

$$g(v_c, v) = 0.5(\tanh(b(v_c - v)) + 1)\,, \tag{3}$$

to represent the effect of the critical vegetation cover described above. It is important to note that using other forms of $g(v_c, v)$ will not change the main results of the model as long as the above destructive effect decreases with vegetation cover or when the erodible gaps between plants decrease in size [*Okin*, 2008].

The third term in Eq. (1), $-\gamma \mathrm{DP}^{2/3} v$, stands for vegetation suppression due to direct wind action, which increases evapotranspiration, uproots, erodes, and suppresses vegetation growth [*Hesp*, 2002]. The two thirds power aims in representing the wind drag on vegetation which is proportional to the square [*Bagnold*, 1941] of the wind speed U (while DP$\propto U^3$). This term is proportional to v, as it is a mortality term. γ is a proportionality constant that depends on vegetation types. The fourth term in Eq. (1), $-\mu v$, stands for an extinction rate due to human activity, such as grazing, clear-cutting or burning, governed by the value of the parameter μ.

The last three terms in Eq. (1) describe the spatial dynamics of the vegetation cover acting in regions with spatial variability in vegetation cover. The fifth term in the RHS of Eq. (1) describes vegetation response to sand flux in regions where $\nabla v \neq 0$. Sand flux through an area element, $\Delta x \times \Delta y$, is proportional to $\mathrm{DP}g(v_c, v)$. We first develop the net sand flux (due to sand erosion or deposition) along the x direction—it is proportional to $\Delta y[\mathrm{DP}g(v_c, v)|_{x+\Delta x} - \mathrm{DP}g(v_c, v)|_x]$. Taking the limit $\Delta x \to 0$ and invoking the definition of the partial derivative leads to $\Delta x \Delta y \partial_x [|\mathrm{DP}g(v_c, v)|]$; we use the absolute value as this term is always associated with decrease in vegetation. When including also the y direction this term is generalized to $\Delta x \Delta y \mathrm{DP} \left|(\partial g/\partial v)\nabla v \cdot \vec{k}\right|$ where $\vec{k}$ is a unit vector along the wind direction. Below we assume uniform wind direction and thus DP is not affected by the differentiation operation. Using: (i) the chain rule on $g(v_c, v)$, (ii) the fact that $g(v_c, v)$ is a monotonic decreasing function of v, and (iii) applying the erosion/deposition effect only along the wind direction, $\vec{k}$, lead to $\Delta x \Delta y DP(\partial g/\partial v) \left|\nabla v \cdot \vec{k}\right|$. Finally, using a proportionality constant, β, and assuming that this suppression term is proportional to v, we obtain $\beta \mathrm{DP} \frac{\partial g(v_c,v)}{\partial v} \left|\nabla v \cdot \vec{k}\right| v$. Using $g(v_c, v)$ as given in Eq. (3) we get

$$\frac{\partial g(v_c, v)}{\partial v} = -\frac{b}{2}\mathrm{sech}^2\left(b(v_c - v)\right). \tag{4}$$

The sixth term on the RHS of Eq. (1), $-\kappa \mathrm{DP}^{2/3}(\nabla v \cdot \vec{k})v$, represents the spatial direct wind effect on vegetation. When vegetation cover increases along the wind direction (i.e $\nabla v > 0$) , vegetation cover is locally suppressed due to the stronger wind stress effect on the less protected (vegetated) region and since seeds are carried away by the wind from this region. The opposite (vegetation enhancement) occurs for regions at which the vegetation density decreases along the wind direction—wind stress effect in this region is smaller as vegetation at this edge is protected by the more dense region in the upwind

side and as more seeds are transported from the upwind side. The sharper the vegetation gradient the larger this term is and vice versa [*Puigdefábregasa et al.*, 1999]. This term is (i) zero where $\nabla v = 0$, i.e., for uniform vegetation cover, (ii) negative at windward side of a blowout where the vegetation is more exposed to the wind and (iii) positive at the leeward slope where it is more protected from the wind. Thus, this term mimics blowout propagation along the prevailing wind.

The last term of Eq. (1), $\delta\nabla^2 v$, represents an isotropic seed dispersal where δ is a diffusion coefficient. Although the wind can induce long-distance seed dispersal, most of the seeds fall at short distance from the canopy [*Nathan et al.*, 2002], which justifies using a simple diffusion term. The diffusion term acts both parallel and perpendicular to wind direction whereas the former two terms act only along the wind direction.

The proposed model has 13 parameters which are summarized in Table 1. It is possible to reduce the number of independent parameters to 8. Still, we prefer to keep the model in its present form, to allow easier interpretation of the results. Most of the model's parameters can be estimated from previous works (see [*Yizhaq et al.*, 2009] for more details); Table 1 includes a range of values for each of the model's parameters, based on the literature published on the subject.

3. Results

The model described above can be used to study the development of different vegetation patterns such as vegetated spots within background of sand, sand-vegetation front, and sand spots within background of vegetation. Below we focus on the last two, as these may be linked to geomorphological observations of sand blowouts.

Fig. 3 depicts the model's evolution of a blowout propagating downwind. We choose $p = 700$ mm/yr[1] and DP=425 since these values yield bistability of both active and fixed dunes states in the absence of spatial dynamics, and hence front dynamics is expected to occur when spatial dynamics is included.

The initial blowout area can increase or decrease with time, depending, for example, on DP (keeping the rainfall constant). Fig. 4 shows that the dynamics in the along-wind direction is different from those of the cross-wind direction. For example for DP=450 the along-wind cross section increases with time, whereas the cross-wind cross section decreases but more slowly, resulting in total area increase. Still, it is clear that after a sufficiently long time the blowout will vanish as growth in both directions is necessary for blowout expansion. Such elongated form of blowouts in the wind direction is supported by field observation as shown in Fig. 1.

The dynamics of transgressive duenfields and blowouts is a result of along wind FA and AF fronts dynamics. The FA and AF front velocities, v_{FA} and v_{AF}, are mainly dictated by the gradient terms in Eq. (1). Fig. 4 depicts the velocities of these fronts as a function of DP for $p = 700$ mm/y. The initial blowout is growing in the along wind (x) direction when $v_{\mathrm{AF}} > v_{\mathrm{FA}}$. In the cross-wind ($y$) direction the condition for growth is $v_{\mathrm{CW}} < 0$. We denote the DP for which $v_{\mathrm{AF}} = v_{\mathrm{FA}}$ as $\mathrm{DP_W}$ and the DP for which $v_{\mathrm{CW}} = 0$ as $\mathrm{DP_{CW}}$.

According to Fig. 4a it is possible to classify the blowout dynamics into three categories: (i) the blowout is shrinking in both directions, $\mathrm{DP} < \mathrm{DP_w}$, (ii) the blowout is expanding in both directions, $\mathrm{DP} > \mathrm{DP_{CW}}$, and (iii) the blowout is shrinking in the cross-wind direction by growing along the wind direction, $\mathrm{DP_w} < \mathrm{DP} < \mathrm{DP_{CW}}$. It is clear that after a sufficiently long time also category (iii) will result in a diminished blowout. Yet,

within region (iii) when $v_{\rm AF} - v_{\rm FA} > v_{\rm CW}$ the area of the initial blowout may grow despite the fact that after some time it will shrink. A simple analysis for a rectangular blowout with dimensions L_x and L_y yields that $dL_y/dt = -2v_{CW}$ and $dL_x/dt = v_{AF} - v_{FA}$ where we assume that blowout remains rectangular during its evolution. The blowout area $S = L_x L_Y$ can be written as:

$$S(t) = -2v_{CW}ut^2 + (L_{y0}u - 2v_{CW}L_{x0})\,t + S_0\,, \tag{5}$$

where $u = v_{AF} - v_{FA}$ and L_{x0}, L_{y0} and S_0 are the initial dimensions and area of the blowout; see Fig. 4. According to Eq. 5, the blowout area evolution follows a quadratic growth (see Fig. 3b). Maximum area will occur at $t_{\rm max} = (L_{y0}u - 2v_{CW}L_{x0})/4v_{CW}u$. The area of the large blowouts increases initially although finally they are predicted to vanish. In addition, small or elongated (along-wind) blowouts shrink faster (compare to squared ones of the same area) [*Levin*, 2011], as seems to be the case for the blowouts from Fraser Island shown in Fig. 2, and numerically in Fig. 5d and Fig. 6.

By using the time series of climate data (annually averages) for Fraser island and despite the uncertainty in the parameters values, the model can show the blowout evolution with a variable climate. Fig. 7 shows the annual DP and rainfall measured at Sandy Cape Lighthouse meteorological station (24.73°S, 153.21° E) for the years 1957-2006.

Fig. 8 shows the development of two initial blowouts which differ by their initial size according to the climate variables shown in Fig. 7. The blowout dynamics follow the climatic trend, but it is more smooth as the vegetation cover response time is large and can not change abruptly to follow the erratic behavior of DP and p. We observe fast growth of the initial blowout till 1982 and then its growth stopped and even decreased following the decrease in DP between 1982-2006, in agreement with the data from Fraser

island (Fig. 3). Note that the area of the larger blowout increased much faster than the smaller one.

4. Conclusions

We have developed a model for the spatial dynamics of vegetation cover on sand. Based on this model we suggest conditions for the growth and shrink of blowouts (depending on wind power and precipitation). We highlight the possibility of transient growth of a blowout that eventually shrink with time—larger blowouts experience a longer transient growth time. In agreement with field observations, the larger the initial blowout is the faster it grow while small and/or elongated blowouts shrink faster. The blowout propagation is a consequence of the difference in along/cross wind fronts velocities. Thus, changes in rainfall and wind power can change blowouts and transgressive dune dynamics. We show that blowout has long response time and that year to year variability (and obviously inter-annual variability) is filtered out due to this long response time. Prolonged droughts or an increase in DP can lead to development of blowouts which will increase the overall dune activity.

Acknowledgments. We thank the Israel Science Foundation for financial support.

Notes

1. The results will be almost the same for $p > 700$ mm/yr as for large rainfall amounts the growth rate convergence to a maximal value.

References

Andreotti, B., P. Claudin, and S. Douady (2002), Part 2: A two-dimensional modeling, *Eur. Phys. J*, *28*, 341–352.

Bagnold, R. A. (1941), *The physics of blown sands and desert dunes*, Chapmann and Hall, London.

Bullard, J. E. (1997), A note on the use of the "Fryberger method" for evaluating potential sand transport by wind, *J. Sedimentary Res.*, *67*(3), 499–501.

Durán, O., and H. J. Herrmann (2006), Vegetation against dune mobility, *Phys. Rev. Lett.*, *97*, 188,001.

Field, J. P., J. Benlap, D. D. Breshears, J. C. Neff, G. S. Okin, J. J. Whicker, T. H. Painter, S. Ravi, M. C. Reheis, and R. L. Reynolds (2010), The ecology of dust, *Front Ecological Environment*, *8*(8), 423–430.

Fryberger, S. G. (1979), Dune forms and wind regime, in *A study of global sand seas*, vol. 1052, edited by E. D. McKee, pp. 137–169, U.S. Geol. Surv.

Hesp, P. A. (2002), Fordunes and blowouts: initation geomorphology and dynamics, *Geomorphology*, *48*, 245–268.

Hesp, P. A., and M. L. Martínez (2007), *Disturbunce Processes and Dynammics in Coastal Dunes*, chap. Plant Disturbance Ecology, pp. 215–247, Elsevier, Amsterdam.

Hugenholtz, C. H., and S. A. Wolfe (2005), Biogeomorphic model of dunefield activation and stabilization on the northern Great Plains, *Geomorphology*, *70*(1-2), 53–70.

Kalnay, E., M. Kanamitsu, R. Kistler, W. Collins, D. Deaven, L. Gandin, M. Iredell, S. Saha, G. White, J. Woollen, Y. Zhu, M. Chelliah, W. Ebisuzaki, W. Higgins, J. Janowiak, K. C. Mo, C. Ropelewski, J. Wang, A. Leetmaa, R. Reynolds, R. Jenne,

and D. Joseph (1996), The NCEP/NCAR 40-year reanalysis project, *Bulletin of the American Meteorological Society*, *77*(3), 437–471.

Levin, N. (2011), Climate-driven changes in tropical cyclone intensity shape dune activity on Earth's largest sand island, *Geomorphology*, *125*(1), 239–252.

Luna, M. C. d. M., E. J. R. Parteli, E. Durán, and H. J. Herrmann (2009), Modeling transverse dunes with vegetation, *Physica A*, *388*, 4205–4217.

Martinho, T., P. A. Hesp, and S. R. Dillenburg (2010), Morphological and temporal variations of transgressive dunefields of the northern and mid-littoral Rio Grande do Sul coast, Southern Brazil, *Geomorphology*, *117*, 14–32.

Nathan, R., G. G. Katul, H. S. Horn, S. M. Thomas, R. Oren, R. Avissar, S. W. Pacala, and S. A. Levin (2002), Mechanisms of long-distance dispersal of seeds by wind, *Nature*, *418*, 409–413.

Okin, G. S. (2008), A new model of wind erosion in the presence of vegetation, *J. Geophys. Res.-Earth Surface*, *113*, F02S10.

Puigdefábregasa, J., F. Gallartb, O. Biaciottoc, M. Allogiad, and G. del Barrio (1999), Banded vegetation patterning in a subantarctic forest of Tierra del Fuego, as an outcome of the interaction between wind and tree growth, *Acta Oecologica*, *20*(3), 135–146.

Pye, K. (1982), Morpholgical development of coastal dunes in a humid trophical environment, cape bedford and cape flattery, north queensland, *Geografiska Annaler. Series A. Physical Geography*, *64*, 213–227.

Reitz, M. D., D. J. Jerolmack, R. C. Ewing, and R. L. Martin (2010), Barchan-parabolic dune pattern transition from vegetation stability threshold, *Geophys. Res. Lett.*, *37*, L19,402.

Shmida, A., M. Evenari, and I. Noy-Meir (1986), Hot desert ecosystems: an integrated view, in *Ecosystems of the world 12B. Hot desert and arid shrublands*, edited by M. Evenari, I. Noy-Meir, and D. Gooddall, pp. 379–387, Elsevier, Amsterdam.

Tsoar, H. (2005), Sand dunes mobility and stability in relation to climate, *Physica A*, *357*(1), 50–56.

Uppala, S. M., P. W. Kallberg, A. J. Simmons, U. Andrae, V. da Costa Bechtold, M. Fiorino, J. K. Gibson, J. Haseler, A. Hernandez, G. A. Kelly, X. Li, K. Onogi, S. Saarinen, N. Sokka, R. P. Allan, E. Andersson, K. Arpe, M. A. Balmaseda, A. C. M. Beljaars, L. van de Berg, J. Bidlot, N. Bormann, S. Caires, F. Chevallier, A. Dethof, M. Dragosavac, M. Fisher, M. Fuentes, S. Hagemann, E. Holm, B. J. Hoskins, L. Isaksen, P. A. E. M. Janssen, R. Jenne, A. McNally, J.-F. Mahfouf, J.-J. Morcrette, N. A. Rayner, R. W. Saunders, P. Simon, A. Sterl, K. E. Trenberth, A. Untch, D. Vasiljevic, P. Viterbo, and J. Woollen (2005), The ERA-40 re-analysis, *Quart. J. Roy. Meteor. Soc.*, *131*, 2961–3012.

Wolfe, S. A., and W. C. Nickling (1993), The protective role of sparse vegetation in wind erosion, *Prog. Phys. Geog.*, *17*, 50–68.

Wolfe, S. A., and W. C. Nickling (1996), Shear stress partitioning in sparsely vegetated desert canopies, *Earth Surface Processes and Landscape*, *21*, 607–619.

Yizhaq, H., Y. Ashkenazy, and H. Tsoar (2007), Why do active and stabilized dunes coexist under the same climatic conditions?, *Phys. Rev. Lett.*, *98*, 188,001.

Yizhaq, H., Y. Ashkenazy, and H. Tsoar (2009), Sand dune dynamics and climate change: A modeling approach, *J. Geophys. Res.*, *114*, F01,023.

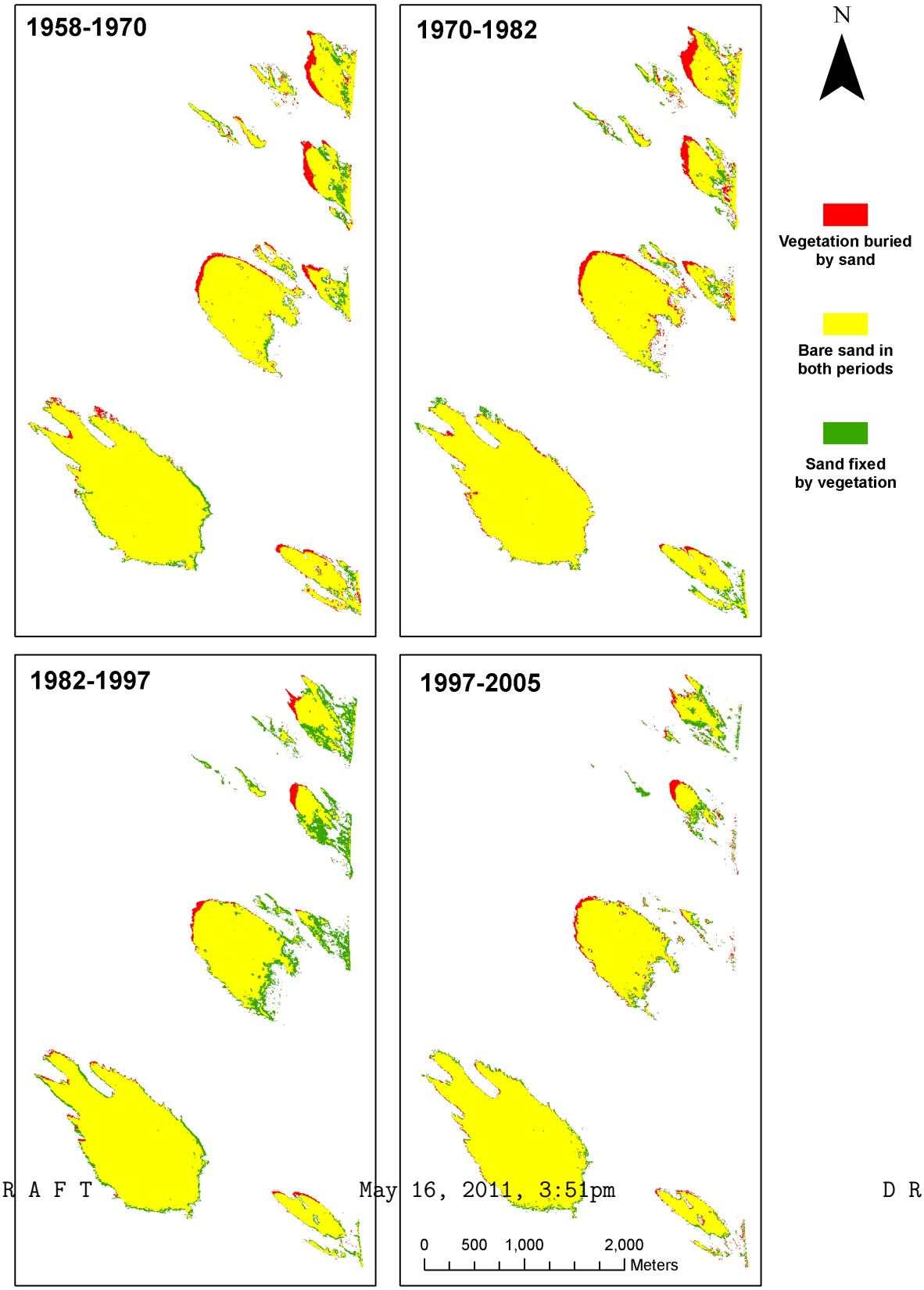

Figure 1. Time evolution of blowouts in Fraser Island, Australia between 1958-2005,

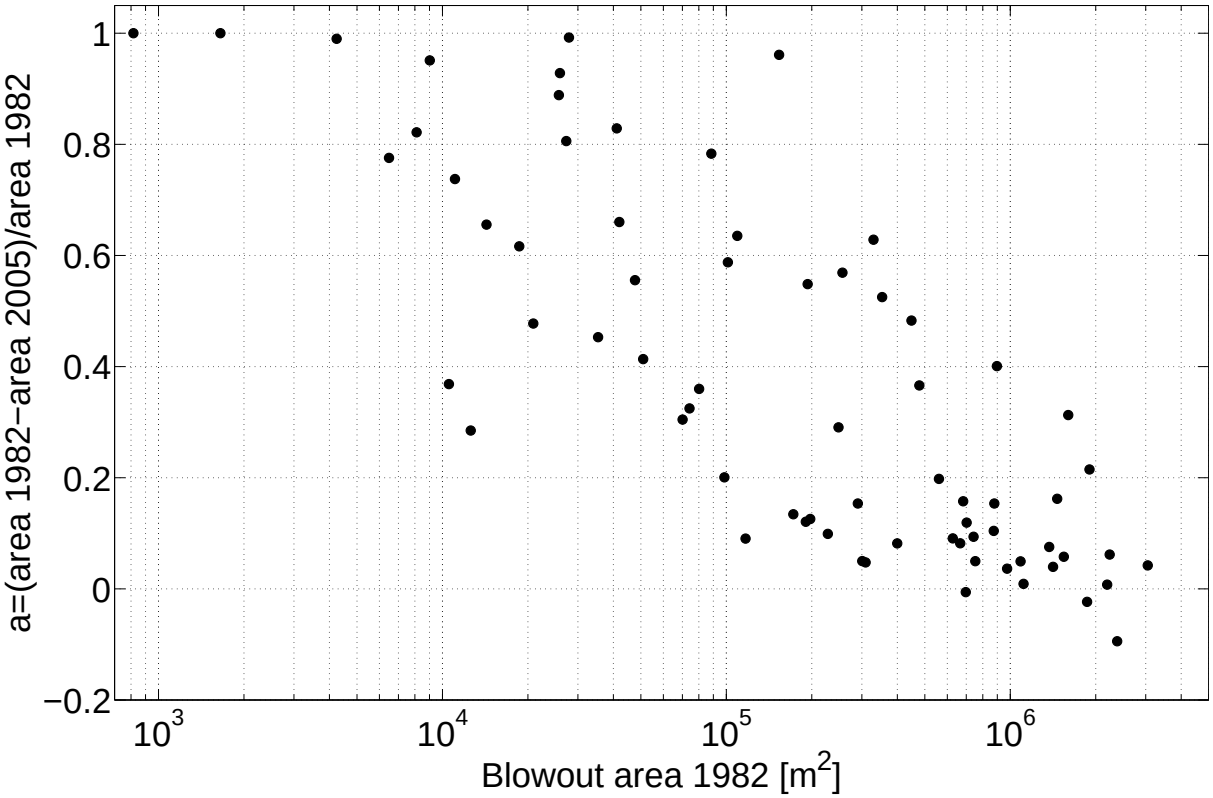

Figure 2. Dune field area changes in Fraser Island during 1982-2005; y-axis shows a normalized change of the area during this period. Negative (positive) values denote blowouts which their areas increased (decreased) in time. The overall trend revealed is of dune stabilization, most probably, due to a significant decrease in wind power during the last three decades.

Parameter	Interpretation	Range
$\alpha_{\max}$	Maximum vegetation cover growth rate	0.1-0.2
$p_{\min}$	Minimal precipitation needed for vegetation growth	50 mm/yr
c	Vegetation growth response to precipitation	50-300 yr^{-1}
η	Spontaneous growth cover	0-0.2
$v_{\max}$	Maximum vegetation cover	0-1
v_c	Critical vegetation cover	0.11-0.35
b	Steepness of transition between interference flow and skimming flow	5-20
μ	Human impact parameter	0-0.1
ε	Vegetation tolerance to sand transport	0.005-0.02
γ	Vegetation vulnerability to wind shear stress	0.005-0.02
β	Vegetation tolerance to sand transport per unit area	0.0001-0.02 m^{-2}
κ	Vegetation vulnerability to wind shear stress at the fronts	0.005-0.02
δ	Vegetation diffusion coefficient	0.1-1 m^2/yr

Table 1. Definition and typical values of the model's parameters. For more details

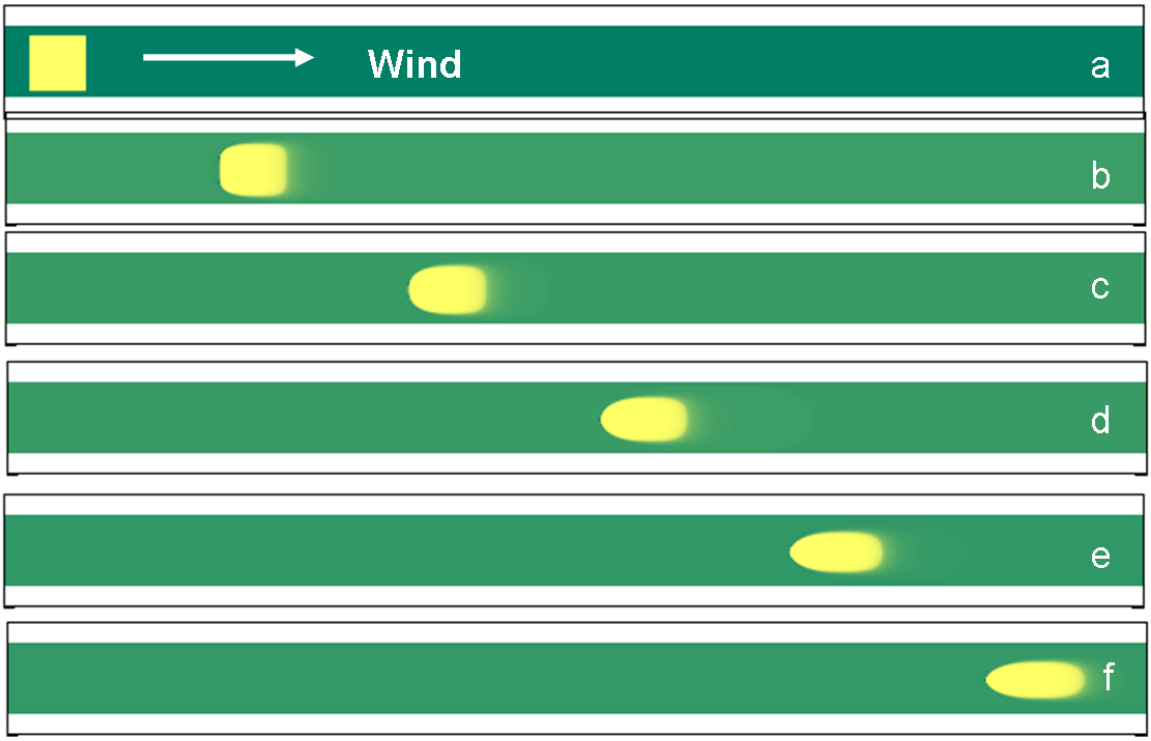

Figure 3. Three hundred years model evolution of a sand spot (yellow) in the background of vegetation (green). The initial blowout (a) propagates downwind with a constant speed that is much higher than the front speed perpendicular to the wind. Panels (b, c, d, e) depict the blowout evolution at 60 years successive intervals. In Fig. 4 we show in details the spatial dynamics of this blowout. Parameters values used: $\alpha_{\max} = 0.15$, $\beta = 6.64 \cdot 10^{-4}$, $\gamma = 0.0008$, $\delta = 0.2$, $\eta = 0.2$, $\kappa = 0.1$, $\mu = 0$, $b = 15$, $c = 100$, $v_c = 0.3$, $v_{max} = 1$ where for this simulation, $p = 700$ mm/y, DP=425, and the spatial initial dimension of the blowout is 50×800 m.

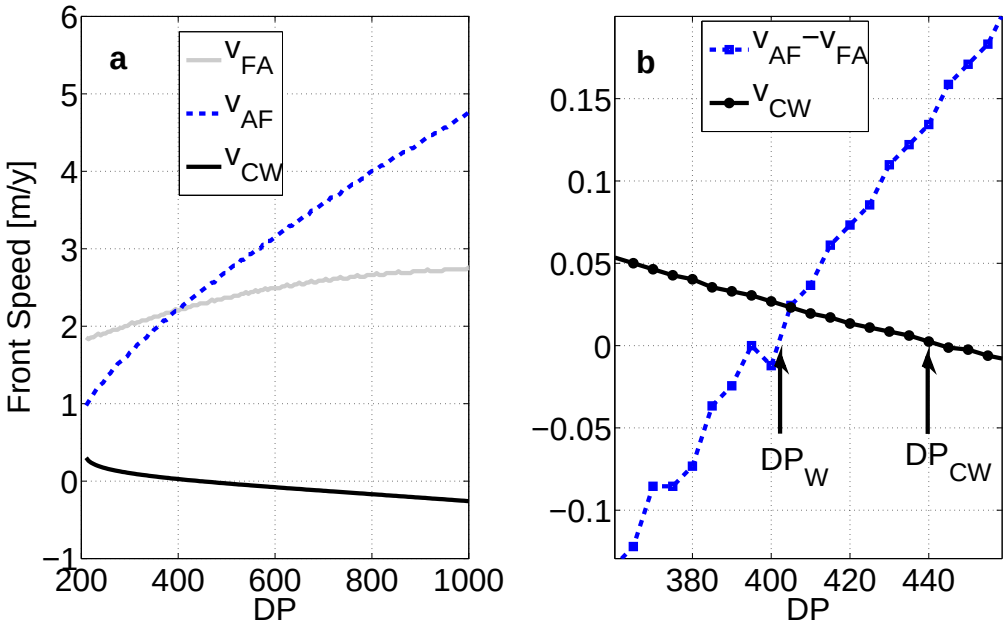

Figure 4. (a) Fronts velocities (v_{AF}, v_{FA}, v_{CW}), as a function of DP for $p = 700$. (b) $v_{\mathrm{AF}} - v_{\mathrm{FA}}$ and v_{CW} as a function of DP. The DP for which $v_{\mathrm{AF}} = v_{\mathrm{FA}}$ is defined as $\mathrm{DP_w}$ and the DP for which $v_{\mathrm{CW}} = 0$ as $\mathrm{DP_{CW}}$. For $\mathrm{DP_W} < \mathrm{DP} < \mathrm{DP_{CW}}$ an initial blowout may initially grow (depending on the initial area and geometry), although finally it will diminish. Parameter values are as in Fig. 3.

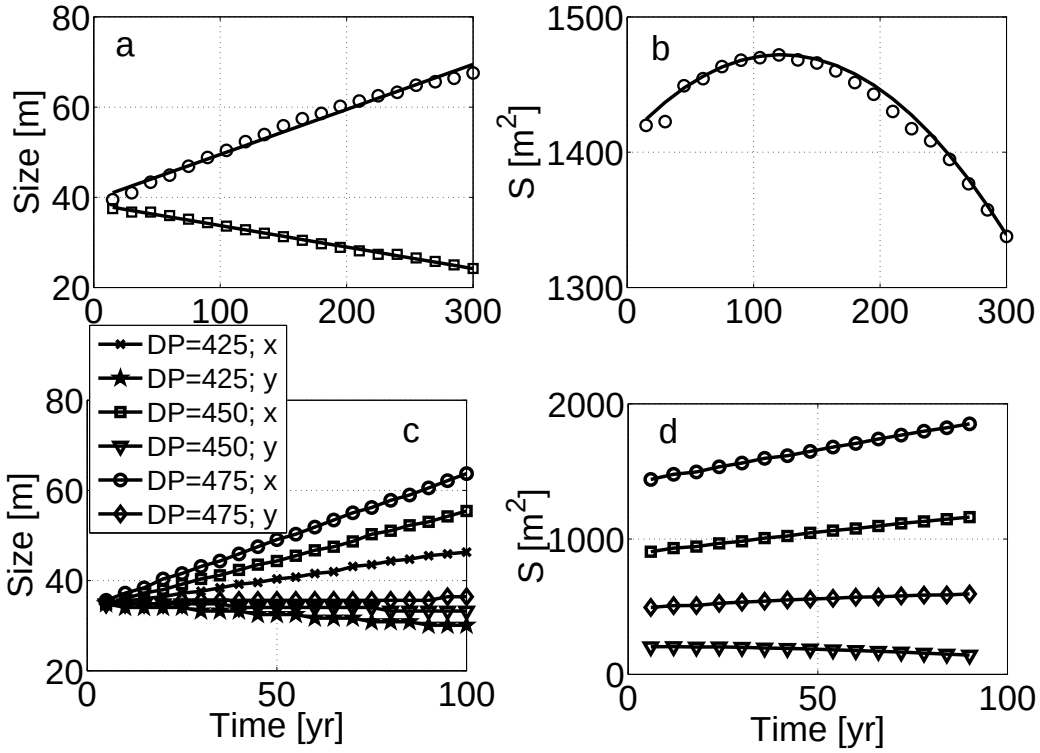

Figure 5. (a) x (circles) and y (squares) blowout dimensions vs. time for the simulation shown in Fig. 2. The solid lines are the linear regressions, indicating growth along the wind direction and shrinkage in the cross-wind direction. (b) Blowout area vs. time showing initial (transient) growth followed by a blowout shrink; the solid line follows the prediction of Eq. 5. (c) Alongwind and crosswind dimensions as a function of time of an initial squared blowout for different values of DP and for $p = 700$ mm/yr. (d) Blowout area as a function of time for different initial square blowout areas (DP=450). Parameters values are as in Fig. 3.

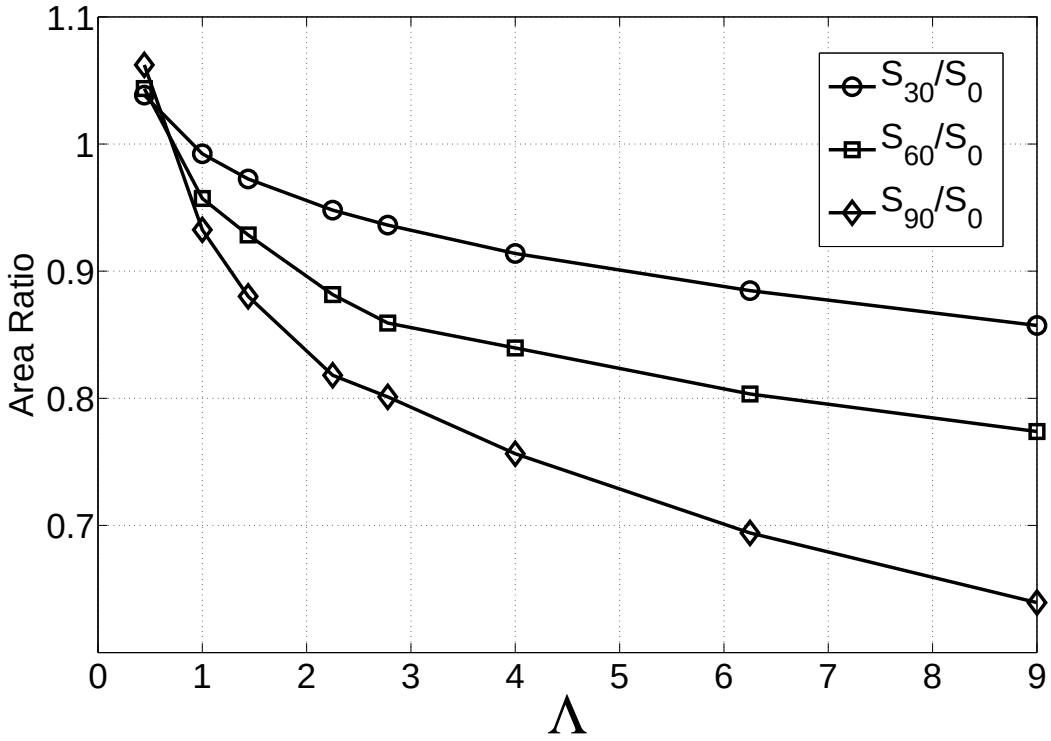

Figure 6. The ratio of the initial blowout area S_0 to the area at 30, 60, 90 years (S_{30}, S_{60}, S_{90}) as the function of the blowout aspect ratio $\Lambda = L_x/L_y$ when the initial blowout area is the same in all simulations. For larger Λ the blowout area shrinks more significantly. Note that for short times and for small Λ the initial area increases. DP=425 and other parameters values are as in Fig. 3.

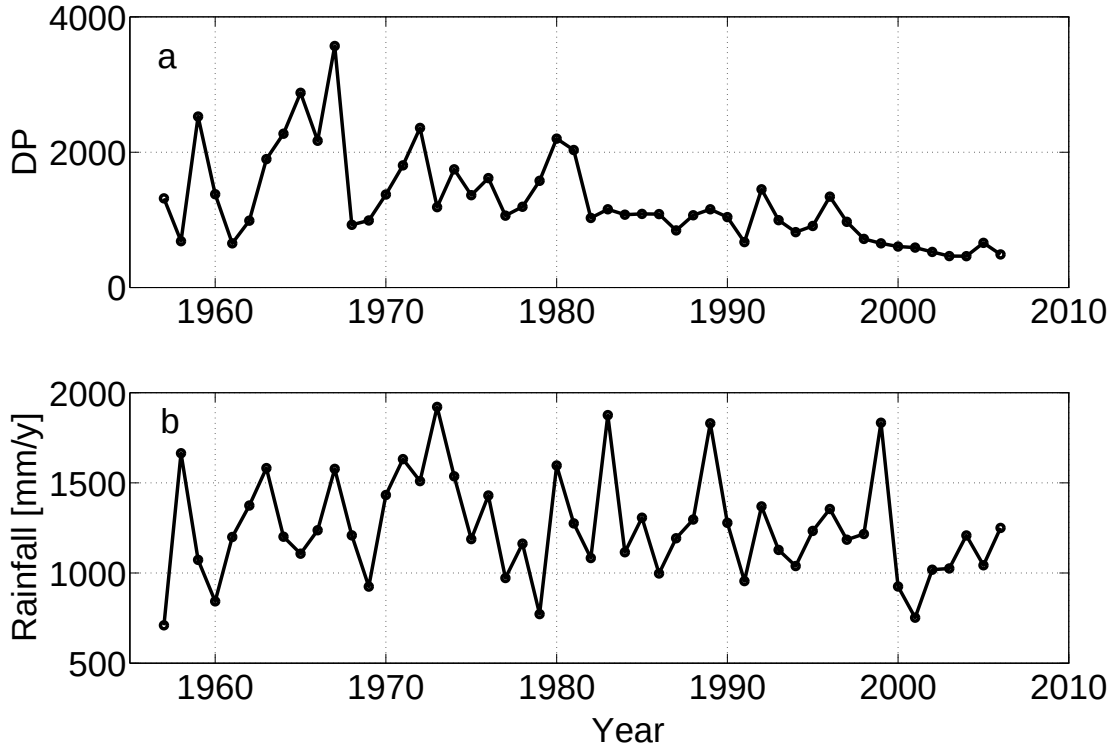

Figure 7. Annual values of DP (a) and rainfall (b) at Sandy Cape lighthouse meteorological station (24.73°S, 153.21°E) near Fraser Island for the years 1957-2006. Note the decline in DP since 1980.

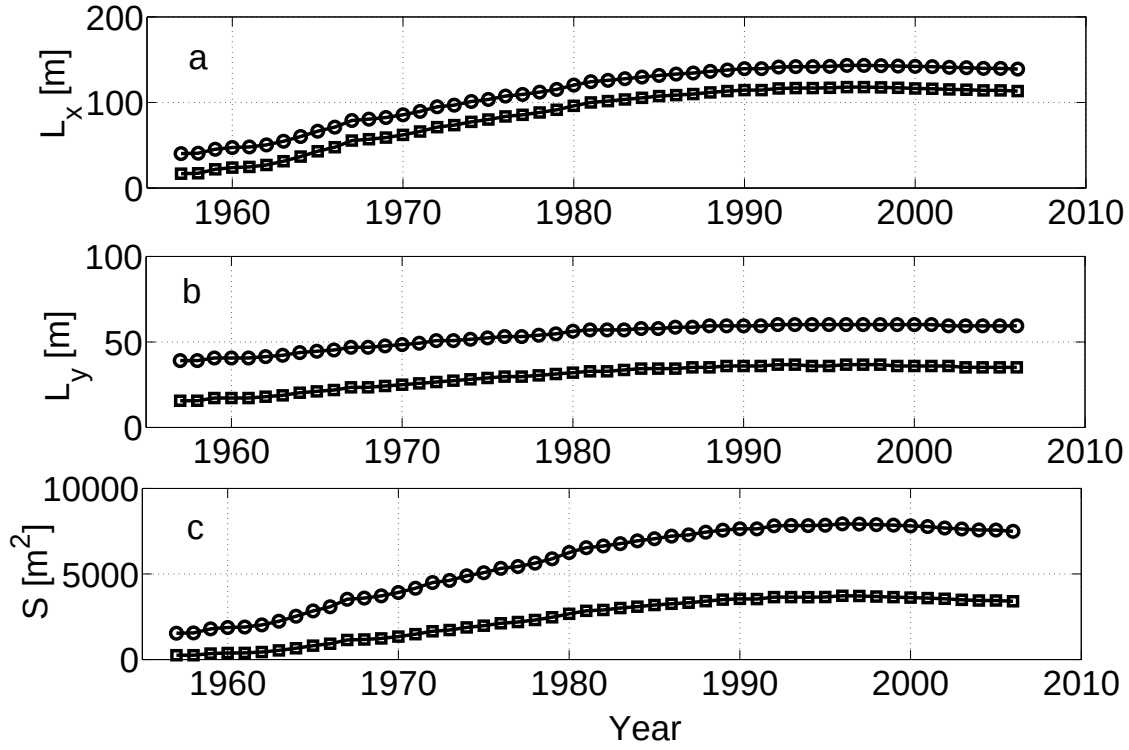

Figure 8. Model simulations for the evolution (alongwind size, L_x, (a); crosswind size, L_y, (b); and area, S, (c)) of two squared blowouts (39×39 m and 16×16 m), forced by the same DP and precipitation depicted in Fig. 7. The fast blowout development almost stopped at 1982 due to the reduction in DP. Parameters values are as in Fig. 3.